

Mobilization efficiency is critically regulated by fat via marrow PPAR δ

Tomohide Suzuki,¹ Shinichi Ishii,¹ Masakazu Shinohara,^{2,3} Yuko Kawano,^{1*} Kanako Wakahashi,^{1*} Hiroki Kawano,^{1*} Akiko Sada,¹ Kentaro Minagawa,^{1**} Michito Hamada,⁴ Satoru Takahashi,^{4,5,6,7} Tomoyuki Furuyashiki,⁸ Nguan Soon Tan,^{9,10} Toshimitsu Matsui¹¹ and Yoshio Katayama¹

¹Hematology, Department of Medicine, Kobe University Graduate School of Medicine, Kobe, Japan; ²Division of Epidemiology, Kobe University Graduate School of Medicine, Kobe, Japan; ³The Integrated Center for Mass Spectrometry, Kobe University Graduate School of Medicine, Kobe, Japan; ⁴Department of Anatomy and Embryology, Faculty of Medicine, University of Tsukuba, Tsukuba, Japan; ⁵Transborder Medical Research Center (TMRC), University of Tsukuba, Tsukuba, Japan; ⁶International Institute for Integrative Sleep Medicine (WPI-IIS), University of Tsukuba, Tsukuba, Japan; ⁷Life Science Center, Tsukuba Advanced Research Alliance (TARA), University of Tsukuba, Tsukuba, Japan; ⁸Division of Pharmacology, Kobe University Graduate School of Medicine, Kobe, Japan; ⁹Lee Kong Chian School of Medicine, Nanyang Technological University Singapore, Singapore; ¹⁰School of Biological Sciences, Nanyang Technological University Singapore, Singapore and ¹¹Department of Hematology, Nishiwaki Municipal Hospital, Nishiwaki, Japan

Current affiliations:

*YKaw and HK: Endocrine/Metabolism Division, Wilmot Cancer Institute, University of Rochester Medical Center, Rochester, NY, USA;

**KW: Area of Cell and Developmental Biology, Centro Nacional de Investigaciones Cardiovasculares Carlos III (CNIC), Madrid, Spain;

**KM: Hematology & Oncology Division, Penn State College of Medicine, Hershey, PA, USA.

©2021 Ferrata Storti Foundation. This is an open-access paper. doi:10.3324/haematol.2020.265751

Received: July 3, 2020.

Accepted: January 19, 2021.

Pre-published: February 4, 2021.

Correspondence: YOSHIO KATAYAMA - katayama@med.kobe-u.ac.jp

Supplementary Appendix

Mobilization efficiency is critically regulated by fat via marrow PPAR δ

Tomohide Suzuki,¹ Shinichi Ishii,¹ Masakazu Shinohara,^{2,3} Yuko Kawano,¹ Kanako Wakahashi,¹ Hiroki Kawano,¹ Akiko Sada,¹ Kentaro Minagawa,¹ Michito Hamada,⁴ Satoru Takahashi,^{4,5,6,7} Tomoyuki Furuyashiki,⁸ Nguan Soon TAN,^{9,10} Toshimitsu Matsui,¹¹ Yoshio Katayama^{1,*}

¹Hematology, Department of Medicine, Kobe University Graduate School of Medicine, 7-5-1 Kusunoki-cho, Chuo-ku, Kobe 650-0017, Japan

²Division of Epidemiology, and ³The Integrated Center for Mass Spectrometry, Kobe University Graduate School of Medicine, 7-5-1 Kusunoki-cho, Chuo-ku, Kobe 650-0017, Japan

⁴Department of Anatomy and Embryology, Faculty of Medicine, ⁵Transborder Medical Research Center (TMRC), ⁶International Institute for Integrative Sleep Medicine (WPI-IIIS), and ⁷Life Science Center, Tsukuba Advanced Research Alliance (TARA), University of Tsukuba, 1-1-1 Tennodai, Tsukuba 305-8576, Japan

⁸Division of Pharmacology, Kobe University Graduate School of Medicine, 7-5-1 Kusunoki-cho, Chuo-ku, Kobe 650-0017, Japan

⁹Lee Kong Chian School of Medicine, Nanyang Technological University Singapore, 11 Mandalay Road, Singapore 308232, and ¹⁰School of Biological Sciences, Nanyang Technological University Singapore, 60 Nanyang Drive, Singapore 637551, Singapore

¹¹Department of Hematology, Nishiwaki Municipal Hospital, 652-1 Shimotoda, Nishiwaki 677-0043, Japan

Supplemental Appendix includes supplemental methods, 1 table, and 12 figures.

*Correspondence:

Yoshio Katayama, MD, PhD

Hematology, Department of Medicine, Kobe University Graduate School of Medicine,
7-5-1 Kusunoki-cho, Chuo-ku, Kobe 650-0017, Japan

Tel: +81-78-382-6912

Fax: +81-78-382-6910

Email: katayama@med.kobe-u.ac.jp

Supplementary Appendix

Supplemental Methods

Generation of PPAR δ ^{-/-} mice

ICR and C57BL/6J mice were purchased from Charles River Laboratories International, Inc. (Yokohama, Japan). Mice were kept in plastic cages under pathogen-free conditions in a room maintained at 23.5±2.5°C and 52.5±12.5% relative humidity under a 14 h light/10 h dark cycle. Mice had free access to commercial chow (MF diet; Oriental Yeast Co., Ltd., Tokyo, Japan) and filtered water. All mouse experiments for the generation of PPAR δ ^{-/-} mice were approved by the University of Tsukuba Animal Experiment Committee.

The mouse genomic sequence (5'-ACG GGG TCC ACG CGT GCG AG-3') in exon 4 of *Ppar δ* was selected as the guide RNA target. This sequence was inserted into the *pX330* plasmid, which carried both guide RNA and Cas9 expression units and was a gift from Dr. Feng Zhang (Addgene plasmid 42230).¹ This *pX330-Ppar δ* DNA vector was isolated with FastGene Plasmid mini kit (Nippon Genetics, Tokyo, Japan) and filtered by Millex-GV® 0.22 μ m filter unit (Merck Millipore, Darmstadt, Germany) for microinjection.

Pregnant mare serum gonadotropin (5 units) and human chorionic gonadotropin (5 units) were intraperitoneally injected into female C57BL/6J mice at 48 h interval and mated with male C57BL/6J mice. Zygotes were collected from the oviducts of mated females, and *pX330-Ppar δ* (circular; 5 ng/ μ L) was microinjected into zygotes. Subsequently, surviving zygotes were transferred into the oviducts of pseudopregnant ICR females, and newborns were obtained.

To confirm the indel mutation induced by CRISPR-Cas9, genomic DNA was purified from the tail. Genomic polymerase chain reaction (PCR) was performed with BioTaq (Bioline, London, UK) and primers (*Ppar δ* -F: 5'-TTG TTT AAC TGC CCC TCC GT-3' and *Ppar δ* -R: 5'-AGG ACT GGA GCT GGG GTA AT-3'). The indel mutation sequence was confirmed with BigDye Terminator v3.1 Cycle Sequencing Kit (Thermo Fisher Scientific, Waltham, MA, USA), FastGene Dye Terminator Removal Kit (Nippon Genetics), and 3500xL Genetic Analyzer (Thermo Fisher Scientific). The random integration of *pX330* was also checked by PCR with *Cas9* gene detecting primers (*Cas9* detection-F: 5'-AGT TCA TCA AGC CCA TCC TG -3', and *Cas9* detection-R: 5'-GAA GTT TCT GTT GGC GAA GC-3').

Generation of chimeric mice

Chimeric (CD45.1/CD45.2) mice were generated by transplantation of 1×10⁶ BM cells from PPAR δ ^{+/+} and PPAR δ ^{-/-} littermate mice (CD45.2) into lethally irradiated (12 Gy, split dose) C57BL/6-CD45.1 congenic mice. Reconstitution by donor cells was confirmed in all recipient mice by blood cell counts. CD45.1/CD45.2 chimerism of peripheral blood leukocytes was assessed by

flow cytometry at 6 weeks after transplantation to ensure that peripheral blood leukocytes were more than 95% of the donor type. Chimeric mice were used for G-CSF mobilization experiments at 8 weeks after transplantation.

Colony-forming units in culture (CFU-C) assay

Mouse HPCs were assayed using methylcellulose-based colony formation medium with growth factors according to the manufacturer's recommendation (Methocult GFM3534; STEMCELL Technologies, Vancouver, BC, Canada).

G-CSF-induced mobilization

Mobilization by G-CSF was induced as described previously.² Briefly, mice were injected with recombinant human G-CSF (Filgrastim; kindly provided by Kyowa Kirin, Tokyo, Japan; 125 µg/kg/dose every 12 h in eight divided doses for 5 days starting on the evening of the first day, s.c.) in PBS supplemented with 0.1% BSA (PBS/BSA). Blood and BM were harvested 3 h after the last dose of G-CSF. In FFD experiments, the same food for each mouse was continued during G-CSF treatment.

The PPAR δ agonist GW501516 (20 mg/kg body weight/day; Cayman Chemical, Ann Arbor, MI, USA) and the PPAR δ antagonist GSK3787 (40 mg/kg body weight/day; Cayman Chemical) were dissolved in 0.5% (w/v) methylcellulose 400 solution (Fujifilm-Wako Pure Chemical Corporation, Osaka, Japan) with 10% dimethyl sulfoxide (Sigma-Aldrich, St. Louis, MO, USA), which was used as vehicle, and administered orally for 5 consecutive days of G-CSF treatment every 24 h in the morning before G-CSF administration. Eicosapentaenoic acid (EPA; 100 µg/mouse/day, MedChemExpress, Princeton, NJ, USA) was dissolved in 200 µL PBS by sonication and intravenously administered for 5 consecutive days of G-CSF treatment every 24 h in the morning before G-CSF administration.

The anti-Angiopoietin-like protein 4 (Angptl4) monoclonal antibody (clone 3F4F5) was generated as described previously³ and intraperitoneally injected twice (20 mg/kg body weight/dose) just before the first and fifth doses of G-CSF. The same amount of IgG from mouse serum (Sigma-Aldrich) was used as vehicle.

Competitive repopulation assay

Stem cell activities of blood mobilized by G-CSF were assessed by long-term competitive reconstitution as described previously⁴ with minor modifications. Briefly, 150 µL mobilized blood (CD45.2) together with 1×10^5 BM nucleated cells from a CD45.1 competitor donor was injected into lethally irradiated (12 Gy, split dose) CD45.1 recipient mice. The proportion of peripheral blood

leukocytes bearing CD45.1 or CD45.2 antigen was determined monthly after transplantation by flow cytometry. Repopulating units (RUs) were calculated using the following standard formula: $RUs = \frac{\%C}{(100-\%)}$, where % is the measured percentage of donor cells (CD45.2⁺ cells derived from mobilized blood) and C is the number of competitor marrow cells per 10⁵, which is 1 in this study.

In vivo depletion of neutrophils

In vivo depletion of mature neutrophils was performed as described previously.² Briefly, mice were injected intraperitoneally with two doses of the anti-Ly6G antibody [200 µg/body/dose; clone 1A8 (LE/AF); Biolegend, San Diego, CA, USA] or rat IgG2aκ isotype control (LE/AF; Biolegend) 9 to 12 h before the initial dose and just before the fourth dose of G-CSF.

Marrow lipid mediator analysis

The quantification of ω3- and ω6-fatty acids and arachidonic acid derivatives in BM was performed as described previously.² Briefly, whole BM of one femur (both BM cells and extracellular fluids; 2 h after eight doses of G-CSF or PBS/BSA) was flushed directly with -20°C 100% methanol and prepared for lipid mediator analysis using LC-MS/MS (QTrap 6500; Sciex, Framingham, MA, USA).

Flow cytometry and cell sorting

Reagents for flow cytometry, including antibodies for the biotin-anti-mouse lineage panel [CD11b, Gr-1 (clone RB6-8C5), Ter119, CD3e, and B220], FITC-anti-Sca-1, and PE-anti-c-kit, were from BD PharMingen (San Diego, CA, USA). PE-Cy5-streptavidin, biotin-anti-F4/80, and APC-streptavidin were from eBioscience (San Diego, CA, USA). FITC-anti-Ly6G (clone 1A8), FITC-anti-CD45.2 and PE-anti-CD45.1 were from BioLegend.

Cells were suspended in 0.5% BSA/2 mM EDTA/PBS and stained for surface markers. For intracellular PPARδ detection, cells were first stained for surface markers, fixed with 2% paraformaldehyde/PBS for 10 min, and permeabilized with 0.1% saponin/PBS for 30 min on ice. Cells were stained with the rabbit anti-PPARδ polyclonal antibody (ab23673; Abcam, Cambridge, MA, USA) at 1:200 dilution or normal rabbit IgG (PM035; MBL, Nagoya, Japan) as control in 10% normal goat serum (Jackson ImmunoResearch Labs, West Grove, PA, USA)/PBS for 30 min followed by incubation with the Alexa Fluor 555 F(ab')₂ fragment of goat anti-rabbit IgG (H+L) for 30 min on ice. Cell analyses were performed on an Accuri C6 flow cytometer (BD Biosciences, San Jose, CA, USA). Data analysis was performed using FlowJo software (FlowJo LLC, Ashland, OR, USA).

For sorting of BM mature neutrophils (CD11b⁺Ly6G^{high}F4/80^{low}), immature neutrophils (CD11b⁺Ly6G^{dull}F4/80^{low}), and monocytes/macrophages (CD11b⁺Ly6G^{dull}F4/80^{high}), BM cells were suspended in 0.1% BSA/2 mM EDTA/PBS and stained with PE-Cy7-anti-CD11b (BD PharMingen),

FITC-anti-Ly6G (Biolegend), and biotin-anti-F4/80 (BD PharMingen) followed by APC-streptavidin. B and T lymphocytes were obtained by staining BM cells with PE-anti-CD45R/B220 (Biolegend) and PE-anti-CD3e (Biolegend), respectively. Nonhematopoietic cells (CD45⁻Ter119⁻) were obtained by staining with APC-anti-Ter119 (Biolegend) and PE-anti-CD45 (BD PharMingen). For the separation of LSK cells, CD117 (c-kit)-positive cells were enriched with anti-mouse CD117 microbeads (Miltenyi Biotech, Gladbach, Germany) and autoMACS separator (Miltenyi Biotech) and stained with the biotin-anti-mouse lineage panel followed by PE-streptavidin (eBioscience), APC-anti-c-kit (BD PharMingen), and FITC-anti-Sca-1 (BD PharMingen). Cell sorting was performed on a MoFlo XDP flow cytometer with Summit software (Beckman Coulter, Brea, CA, USA).

Cell culture for 32D and sorted BM myeloid cells

The neutrophil progenitor cell line 32D was cultured as described previously,² with minor modifications. Briefly, 1×10^6 cells/well were incubated in 500 μ L RPMI 1640 (Sigma-Aldrich) supplemented with 10% fetal bovine serum (FBS) and 15% WEHI-conditioned medium in a 24-well nonculture treatment plate (Falcon®, Corning, Corning, NY, USA) for 12 h at 37°C, 5% CO₂. After acclimatization, indicated concentrations of isoproterenol (DL-isoproterenol hydrochloride; Sigma-Aldrich), G-CSF (Kyowa Kirin), dobutamine hydrochloride (β_1 -AR agonist; Sigma-Aldrich), clenbuterol hydrochloride (β_2 -AR agonist; Sigma-Aldrich), BRL37344 sodium salt hydrate (β_3 -AR agonist; Sigma-Aldrich), GW501516 (Cayman Chemical), GSK3787 (Cayman Chemical), EPA (MedChemExpress), docosahexaenoic acid (DHA; MedChemExpress), α -linolenic acid (α -LA; Santa Cruz Biotechnology, Dallas, TX, USA), and linoleic acid (LA; MedChemExpress) were added. Cultured cells were harvested for mRNA assessment at 3 h for PPAR δ and 12 h for carnitine palmitoyltransferase-1 α (Cpt1 α) and Angptl4.

Sorted BM mature neutrophils (CD11b⁺Ly6G^{high}F4/80^{low}) and immature neutrophils (CD11b⁺Ly6G^{dull}F4/80^{low}) were cultured at a concentration of 4×10^5 cells/well in 500 μ L RPMI 1640 supplemented with 10% FBS and 15% WEHI-conditioned medium in a 24-well nonculture treatment plate (Falcon®; Corning). Monocytes/macrophages (CD11b⁺Ly6G^{dull}F4/80^{high}) were cultured at a concentration of 2×10^5 cells/well in 500 μ L RPMI 1640 supplemented with 10% FBS in a 24-well tissue culture plate (Falcon®; Corning) at 37°C, 5% CO₂ with indicated concentrations of dobutamine, clenbuterol, BRL37344, GSK3787, EPA, and DHA. Cultured cells were harvested for mRNA assessment at 3 h for PPAR δ and 12 h for Cpt1 α and Angptl4.

Tissue preparation and immunohistochemistry

Femoral bone tissues were fixed in 4% paraformaldehyde/PBS at 4°C for 48 h and decalcified in 10% EDTA for 2 weeks at 4°C. For immunohistochemical staining of PPAR δ in BM,

paraffin-embedded sections (4 μm thick) were used. After inhibition of endogenous peroxidase activity with methanol-containing 0.3% hydrogen peroxide for 30 min, antigen retrieval was done with L.A.B.Solution (Polysciences, Warrington, PA, USA). Sections were blocked with 5% goat serum (Jackson Immunoresearch Labs) and 5% FBS/PBS for 1 h. Staining with the rabbit anti-PPAR δ polyclonal antibody (ab23673; Abcam) at 1:200 dilution or normal rabbit IgG (sc-3888; Santa Cruz Biotechnology) as control was visualized using horseradish peroxidase polymer for mouse tissue, HistostarTM (anti-rabbit) mouse immunostaining reagent (MBL, Nagoya, Japan) followed by ImmPACTTM DAB peroxidase substrate kit (Vectorlabs, Burlingame, CA, USA), and hematoxylin staining.

Evans blue dye assay

BM vascular permeability was assessed by Evans blue dye assay as described previously,⁵ with minor modifications. Briefly, 0.5% Evans blue dye (Fujifilm-Wako Pure Chemical Corporation) in 200 μL PBS was injected to 12-week-old mice via tail vein. After 30 min, mice were euthanized and perfused with 30 mL PBS to remove excess Evans blue from the vessels. Femur was flushed with 500 μL ice-cold PBS. BM cells were centrifuged, and the amount of Evans blue in the supernatant was measured at 610 nm in a 96-well plate using an absorbance microplate reader (iMARKTM, Bio-Rad Laboratories, Inc., Hercules, CA, USA).

RNA extraction and quantitative reverse transcription-PCR (qRT-PCR)

Total RNA was extracted with TRIzol solution (Invitrogen, Carlsbad, CA, USA). Total RNA was treated with DNase I (Invitrogen) and reverse transcribed using first-strand cDNA synthesis with random primers (Promega, Madison, WI, USA). qRT-PCR was performed using SYBR Green (Life Technologies, Tokyo, Japan) on a LightCycler 480 System (Roche Diagnostics, Mannheim, Germany). The primers used are listed in Supplemental Table S1. All experiments were done in triplicate and normalized to β -actin or EF1 α .

Enzyme-linked immunosorbent assay (ELISA)

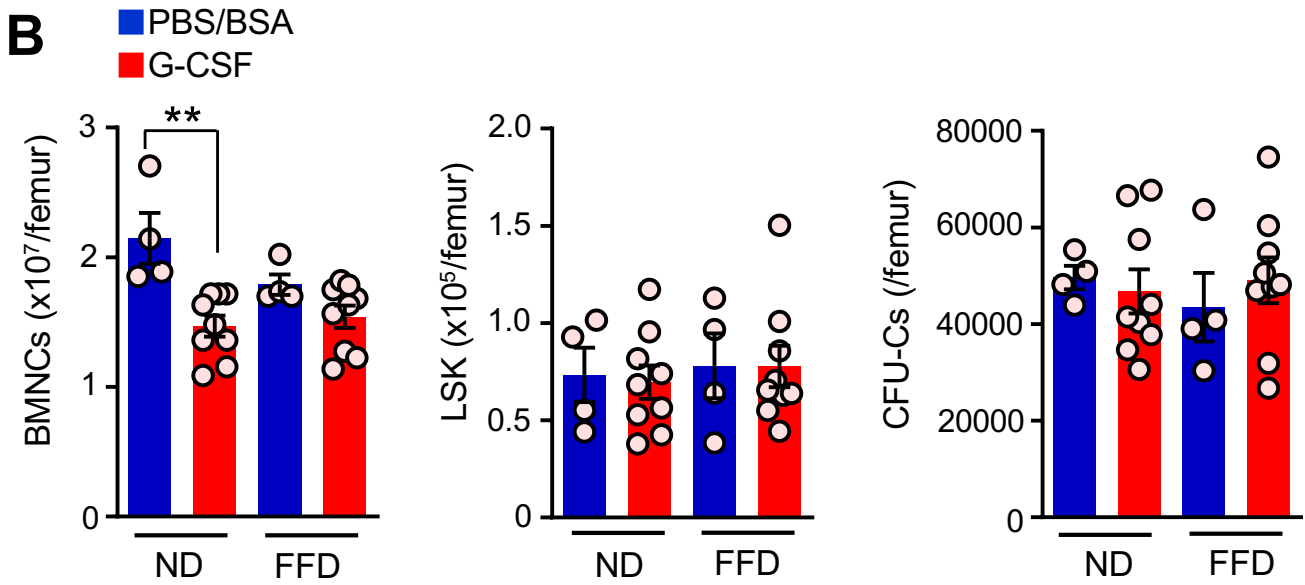
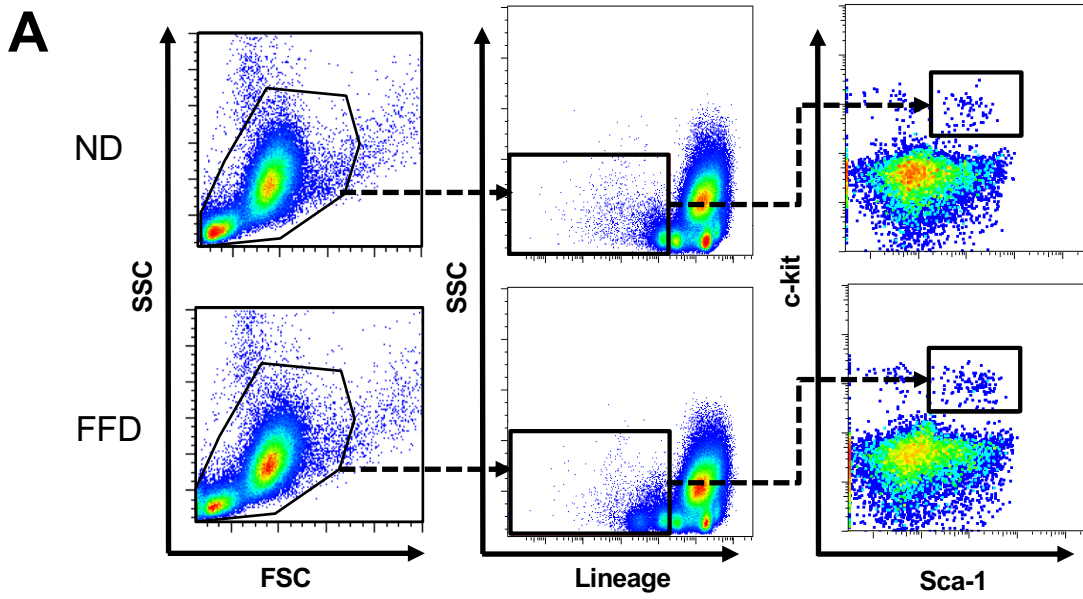
BM extracellular fluid (BMEF) was obtained by flushing femoral BM with 500 μL PBS followed by centrifugation after several pipetting steps. Angptl4 quantification in plasma and BMEF was done using Angptl4 ELISA kit according to the manufacturer's recommendations (MyBioSource, San Diego, CA, USA).

References

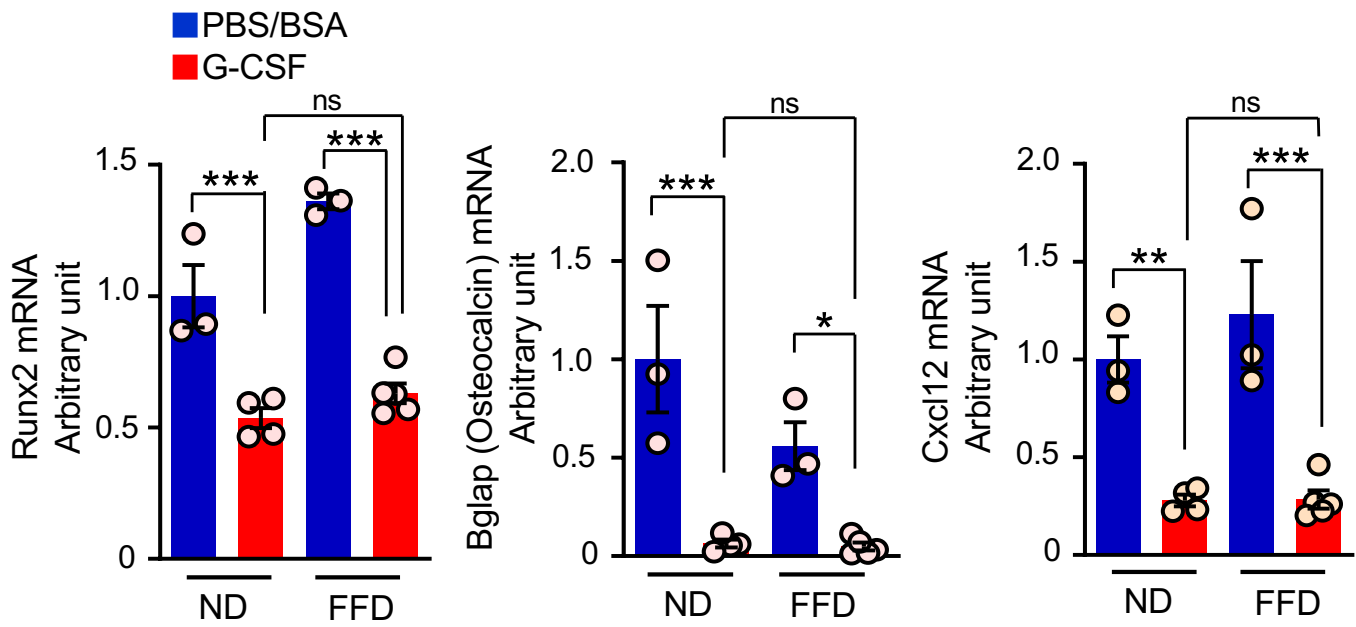
1. Cong L, Ran FA, Cox D, et al. Multiplex genome engineering using CRISPR/Cas systems. *Science*. 2013;339(6121):819-823.
2. Kawano Y, Fukui C, Shinohara M, et al. G-CSF-induced sympathetic tone provokes fever and primes antimobilizing functions of neutrophils via PGE2. *Blood*. 2017;129(5):587-597.
3. Li L, Chong HC, Ng SY, et al. Angiopoietin-like 4 increases pulmonary tissue leakiness and damage during influenza pneumonia. *Cell Rep*. 2015;10(5):654-663.
4. Kawamori Y, Katayama Y, Asada N, et al. Role for vitamin D receptor in the neuronal control of the hematopoietic stem cell niche. *Blood*. 2010;116(25):5528-5535.
5. Bowers E, Slaughter A, Frenette PS, Kuick R, Pello OM, Lucas D. Granulocyte-derived TNF α promotes vascular and hematopoietic regeneration in the bone marrow. *Nat Med*. 2018;24(1):95-102.

Gene	Primer sequence
Ppara	forward 5'-GTCATCACAGACACCCTCTCTCC-3' reverse 5'-ACAGACAGGCACTTGTGAAAAC-3'
Ppard	forward 5'-CCACGAGTTCTTGCGAAGTCTCC-3' reverse 5'-GCAGAAATGGTGCCTGGATGGC-3'
Pparg	forward 5'-TGACAGGAAAGACAACGGACAA-3 reverse 5'-ATCTTCTCCCATCATTAAAGGAATTCAT-3'
Angptl4	forward 5'-CACGCACCTAGACAATGGAGT-3' reverse 5'-AGTCATCTCACAGTTGACCAA-3'
Cpt1a	forward 5'-ATGTCAAGCCAGACGAAGAACATC-3' reverse 5'-CCTTGACCATAGCCATCCAGATTC-3'
β -actin	forward 5'-CTTCTTTGCAGCTCCTTCGTTG-3' reverse 5'-CGACCAGCGCAGCGATATC-3'
Cxcl12	forward 5'-CAA CAC TCC AAA CTG TGC CCT TCA-3' reverse 5'-TCC TTT GGG CTG TTG TGC TTA CT-3'
Runx2	forward 5'- TCC GAA ATG CCT CCG CTG TTA T -3' reverse 5'- GGA CCG TCC ACT GTC ACT TTA A-3'
Bglap (Osteocalcin)	forward 5'-CCC TGA GTC TGA CAA AGC CTT CA-3' reverse 5'-TAG ATG CGT TTG TAG GCG GTC T-3'
Eef1a1 (EF1 α)	forward 5'-GGTTTGCCGTCAGAACGCAG-3' reverse 5'- GTTCGCTTGTCGATTCCACCAC-3'

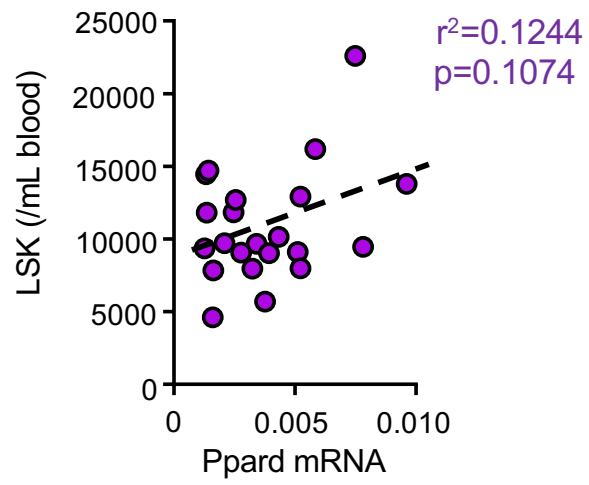
Supplemental Table 1. Primer sequences used for PCR.



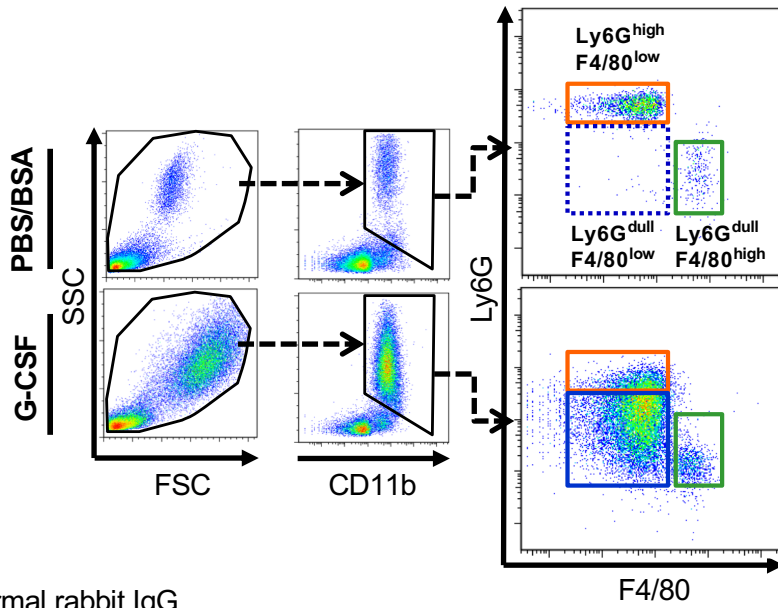
Supplemental Figure 1. Gating strategy for LSK cells in mobilized blood and BM data in G-CSF mobilization experiments related to Figure 1B.



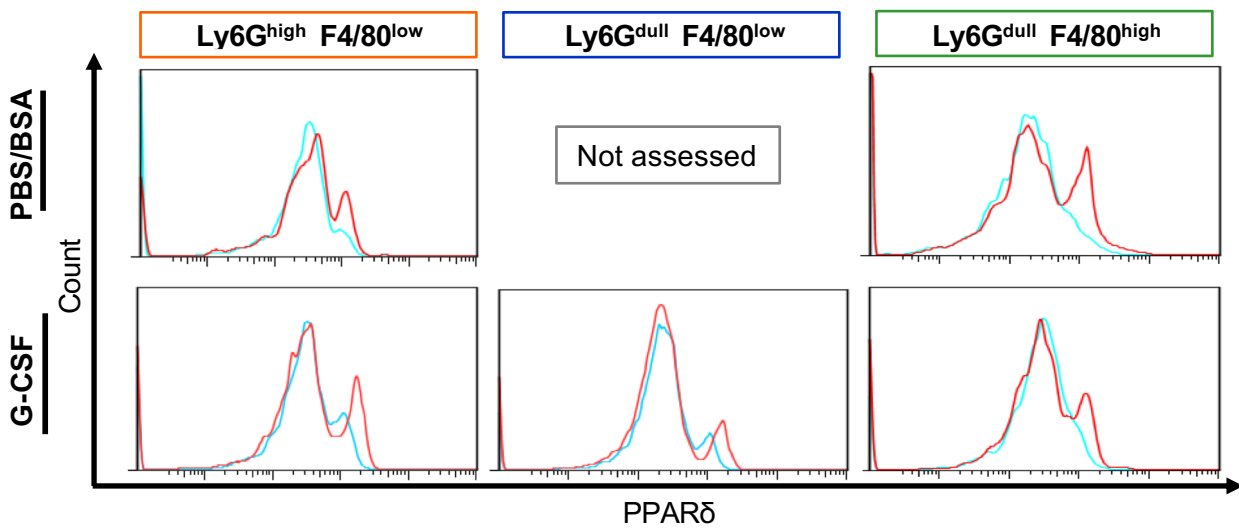
Supplemental Figure 2. BM mRNA expression of mobilization related genes.



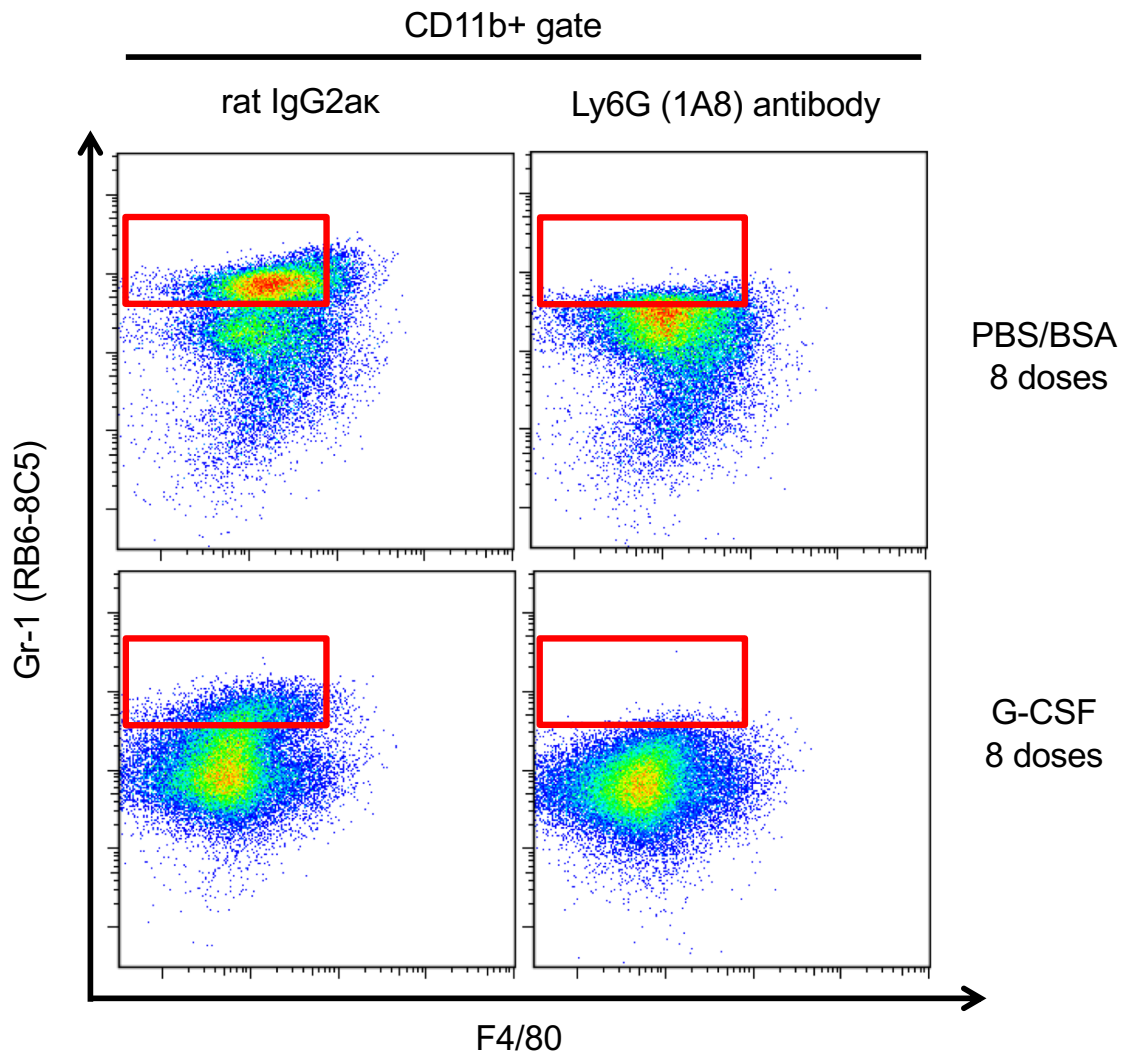
Supplemental Figure 3. Correlation between mobilized LSK cells and BM PPARδ mRNA expression related to Figure 2E.

A**B**

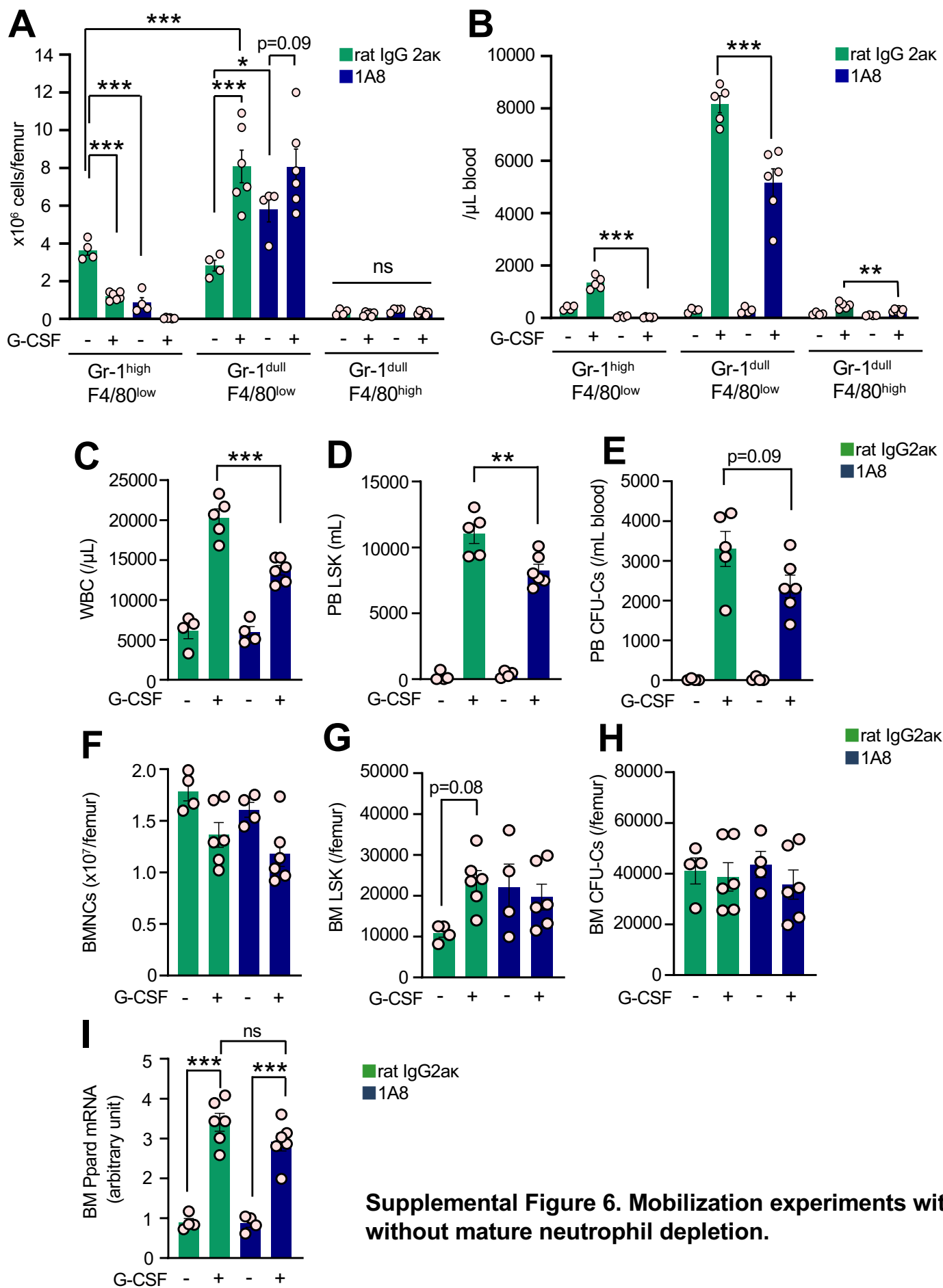
— normal rabbit IgG
 — PPAR δ



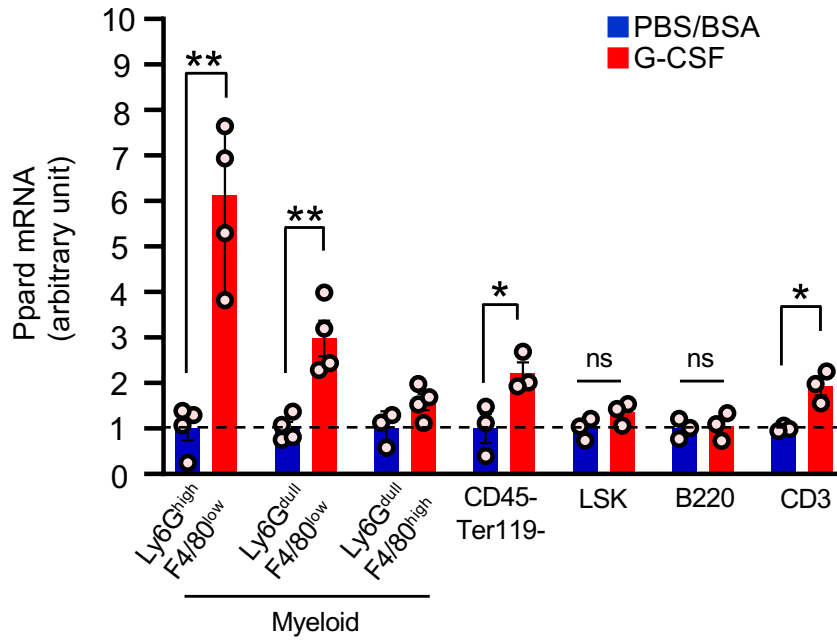
Supplemental Figure 4. PPAR δ protein expression in myeloid cells in peripheral blood.



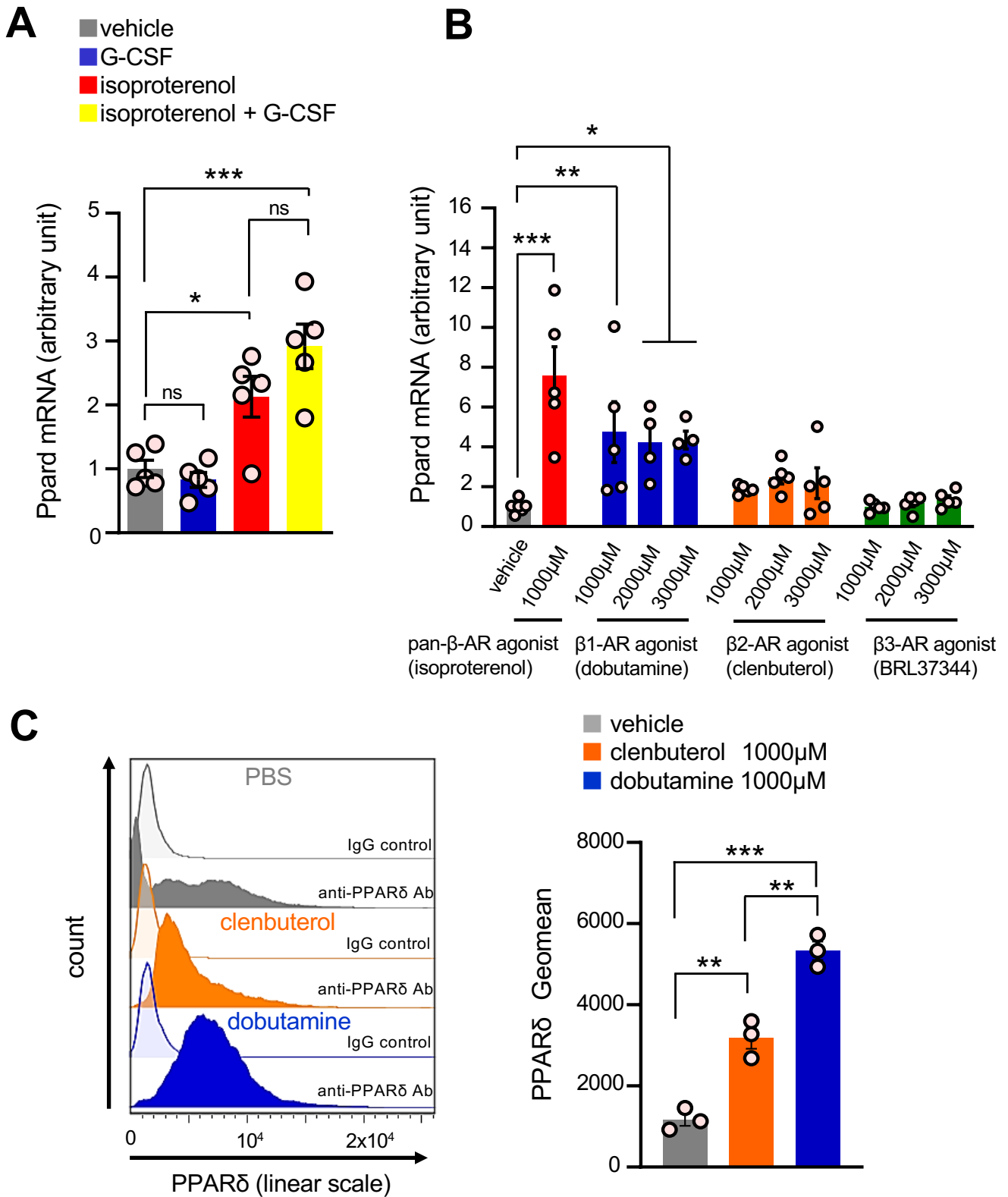
Supplemental Figure 5. Confirmation of mature neutrophil depletion in BM by the anti-Ly6G antibody.



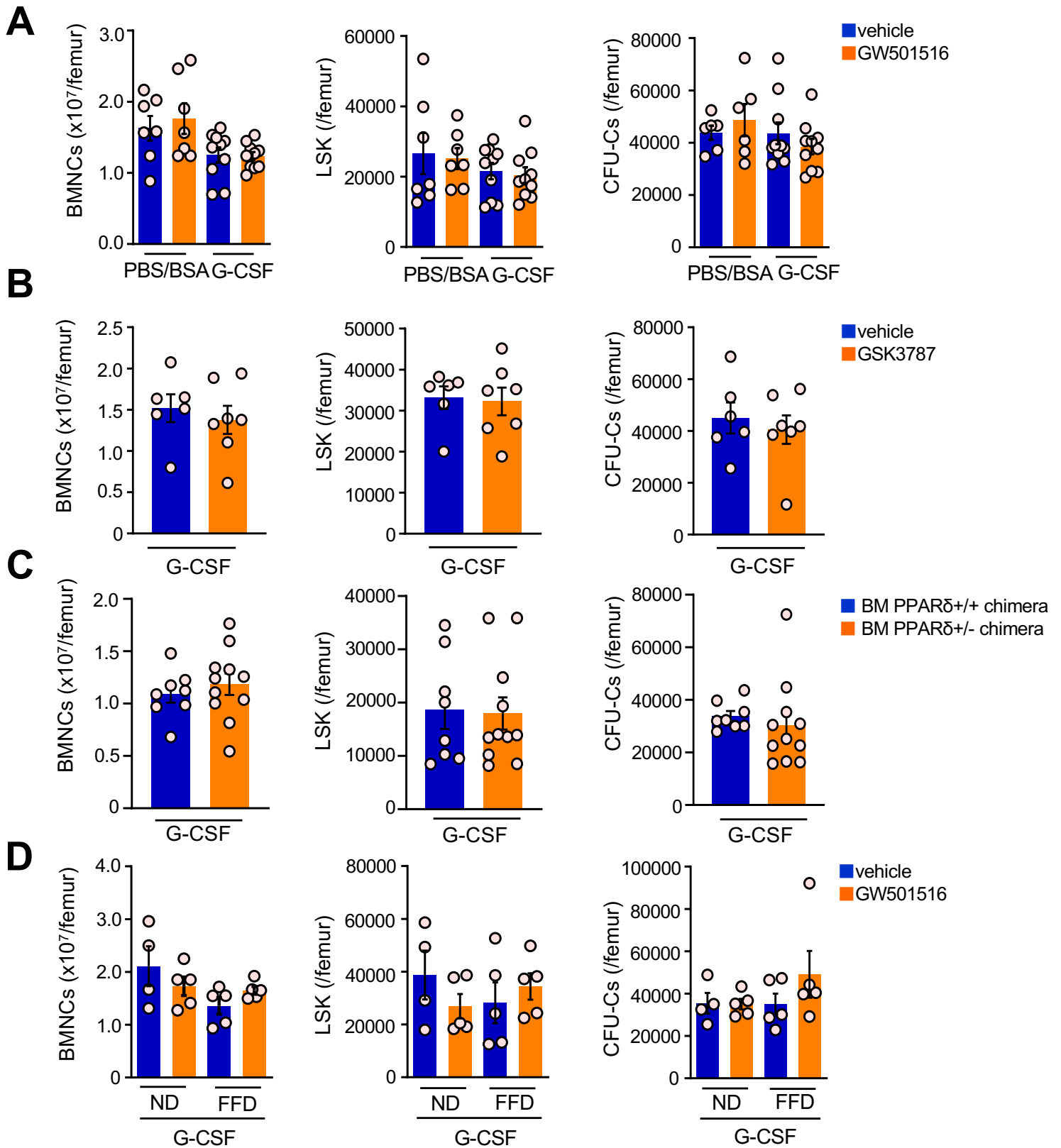
Supplemental Figure 6. Mobilization experiments with or without mature neutrophil depletion.



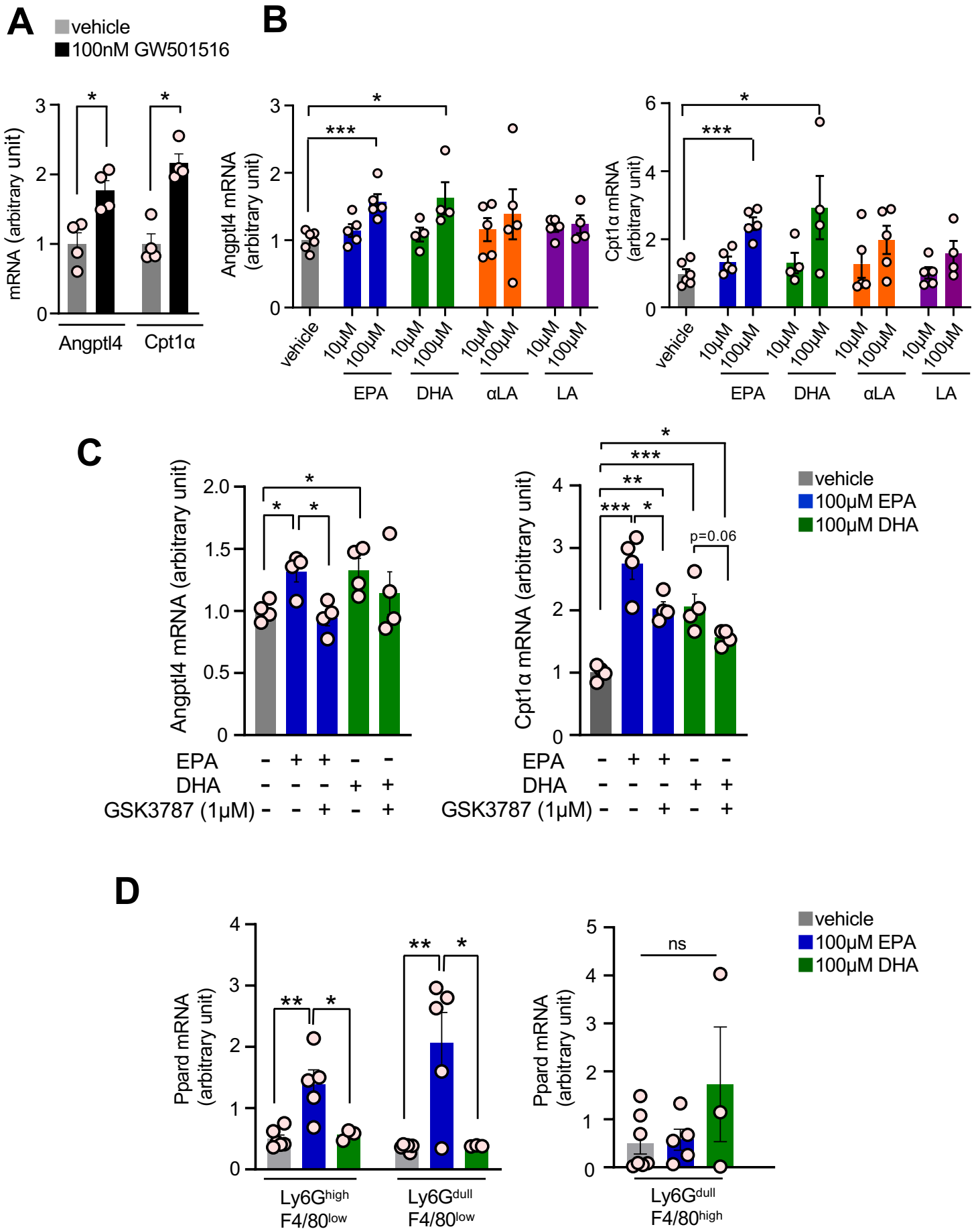
Supplemental Figure 7. Alteration of PPAR δ mRNA expression by G-CSF in myeloid and nonmyeloid BM cell fractions.



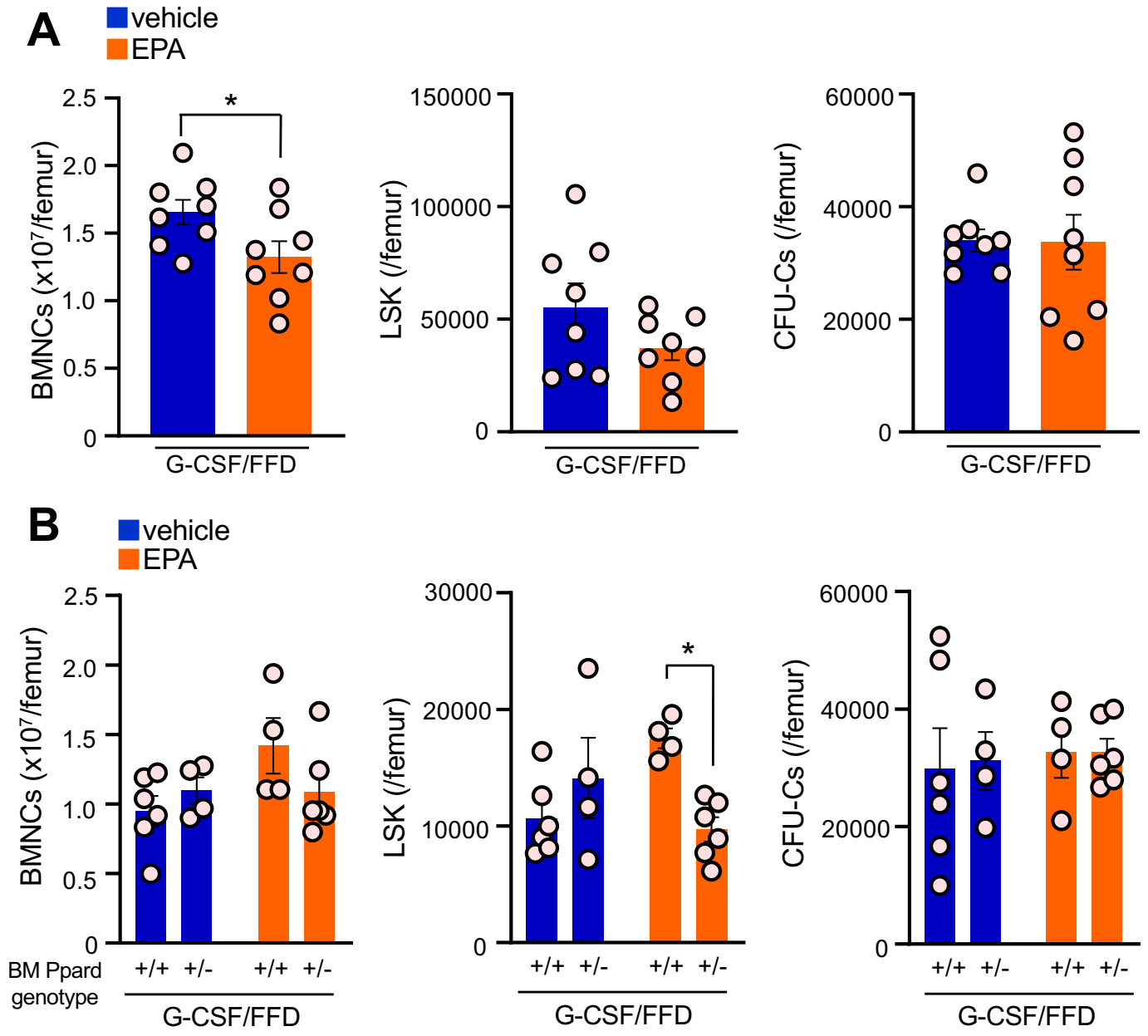
Supplemental Figure 8. Induction of PPAR δ in the 32D neutrophil precursor cell line by β -adrenergic stimulation.



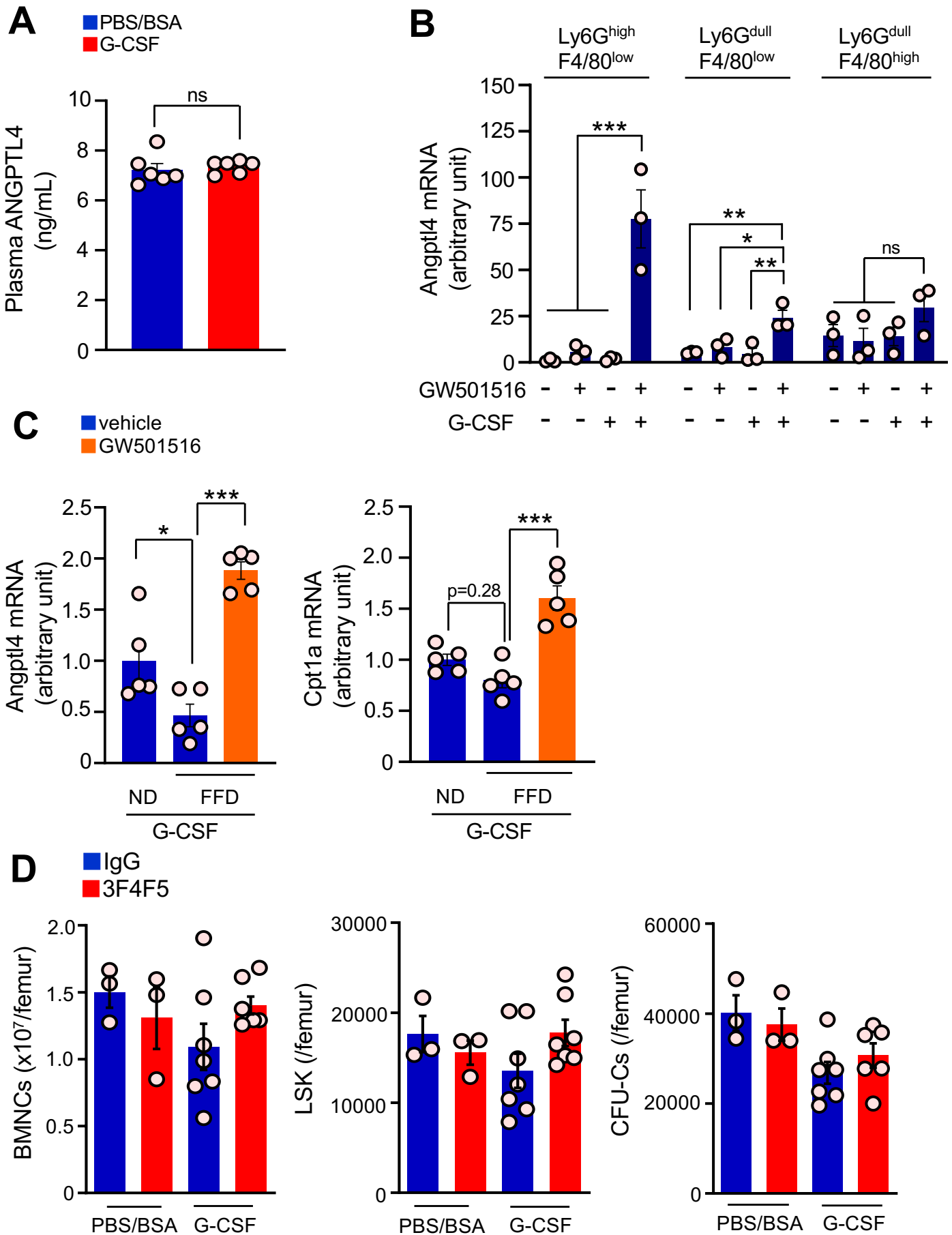
Supplemental Figure 9. BM data in G-CSF mobilization experiments related to Figure 4.



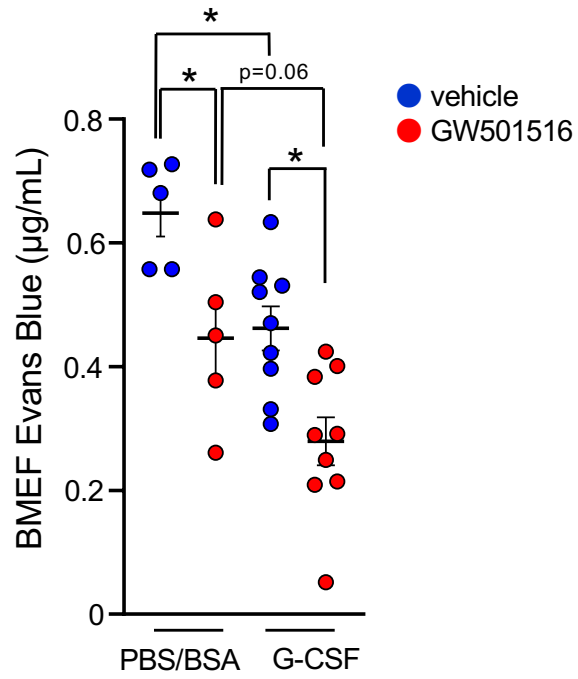
Supplemental Figure 10. Function of ω 3-fatty acids as PPAR δ ligands in vitro.



Supplemental Figure 11. BM data in G-CSF mobilization experiments with EPA treatment related to Figure 6B-C.



Supplemental Figure 12. Expression and function of Angptl4 in G-CSF mobilization.



Supplemental Figure 13. Modulation of BM vascular permeability during G-CSF mobilization by the PPAR δ agonist.

Supplemental Figure Legends

Supplemental Figure 1. Gating strategy for LSK cells in mobilized blood and BM data in G-CSF mobilization experiments related to Figure 1B.

(A) Gating strategy for LSK cells in mobilized blood. (B) BM nucleated cells (BMNCs), LSK, and CFU-Cs in BM (n=4 for PBS/BSA group and n=9 for G-CSF group). ND: normal diet, FFD: fat-free diet. Combined data of at least three independent experiments are shown. Data are mean±SEM. **p<0.01 (ANOVA).

Supplemental Figure 2. BM mRNA expression of mobilization related genes.

Alteration of BM mRNA expression in (A) Runx2, (B) Osteocalcin, and (C) Cxcl12 in mice fed with ND or FFD during G-CSF mobilization (n=3-5). Combined data of three independent experiments are shown. ns: not significant. Data are mean±SEM. *p<0.05, **p<0.01, ***p<0.001 (ANOVA).

Supplemental Figure 3. Correlation between mobilized LSK cells and BM PPAR δ mRNA expression related to Figure 2E.

Correlation of mobilization efficiency of LSK cells in the blood with BM PPAR δ mRNA expression (n=22). Combined data of at least three independent experiments are shown. (Pearson correlation coefficient).

Supplemental Figure 4. PPAR δ protein expression in myeloid cells in peripheral blood.

Flow cytometric analysis of PPAR δ protein expression in three major myeloid cell fractions (CD11b⁺Ly6G^{high}F4/80^{low} mature neutrophils, CD11b⁺Ly6G^{dull}F4/80^{low} immature neutrophils, and CD11b⁺Ly6G^{dull}F4/80^{high} monocytes/macrophages) in the blood after treatment with eight doses of PBS/BSA or G-CSF. (A) Gating strategy and (B) representative histograms of PPAR δ protein expression from three independent experiments are shown.

Supplemental Figure 5. Confirmation of mature neutrophil depletion in BM by the anti-Ly6G antibody.

In vivo depletion of mature neutrophils was performed by intraperitoneal injection with two doses of the anti-Ly6G antibody (200 μ g/body/dose, clone 1A8; 9-12 h before the initial dose and just before the fourth dose of G-CSF). Efficient depletion of BM CD11b⁺Gr-1^{high}F4/80^{low} fraction is shown in both PBS/BSA- and G-CSF-treated groups.

Supplemental Figure 6. Mobilization experiments with or without mature neutrophil depletion.

G-CSF mobilization in mice with or without mature neutrophil depletion. (A-B) Absolute cell

number of each major myeloid cell fraction in (A) BM and (B) blood. (C-H) Mobilization of (C) WBC, (D) LSK, and (E) CFU-Cs in the blood and (F) BMNCs, (G) LSK, and (H) CFU-Cs in BM. (I) BM PPAR δ mRNA expression in G-CSF mobilization with or without mature neutrophil depletion. n=4-6. Combined data of three independent experiments are shown. ns: not significant. Data are mean \pm SEM. *p<0.05, **p<0.01, ***p<0.001 (Student's t test and ANOVA).

Supplemental Figure 7. Alteration of PPAR δ mRNA expression by G-CSF in myeloid and nonmyeloid BM cell fractions.

PPAR δ mRNA expression in sorted myeloid and nonmyeloid BM cell fractions after treatment with eight doses of PBS/BSA or G-CSF. Data are normalized to the mean of the PBS/BSA group of each cell fraction to evaluate the alteration by G-CSF treatment (n=3-4). Combined data of three independent experiments are shown. ns: not significant. Data are mean \pm SEM. *p<0.05, **p<0.01 (Student's t test).

Supplemental Figure 8. Induction of PPAR δ in the 32D neutrophil precursor cell line by β -adrenergic stimulation.

(A-B) PPAR δ mRNA expression in 32D cells treated with (A) G-CSF and/or isoproterenol (n=5) and (B) selective agonists for each β -AR (dobutamine, clenbuterol, and BRL37344 for β_1 -, β_2 -, and β_3 -AR, respectively; n=4-6). (C) Representative histograms and geometric means of PPAR δ protein expression in 32D cells after stimulation with clenbuterol or dobutamine by flow cytometry (n=3). Combined data of three independent experiments are shown. ns: not significant. Data are mean \pm SEM. *p<0.05, **p<0.01, ***p<0.001 (ANOVA).

Supplemental Figure 9. BM data in G-CSF mobilization experiments related to Figure 4.

BMNCs, LSK, and CFU-Cs in G-CSF mobilization experiments in (A) WT mice with the PPAR δ agonist GW501516 (n=6-7 for PBS/BSA group and n=10 for G-CSF group), (B) WT mice with the PPAR δ antagonist GSK3787 (n=6-7), (C) BM PPAR $\delta^{+/-}$ chimeric mice (n=8-11), and (D) WT mice with the PPAR δ agonist GW501516 fed with ND or FFD (n=4-5).

Supplemental Figure 10. Function of ω 3-fatty acids as PPAR δ ligands in vitro.

(A) Up-regulation of Angptl4 and Cpt1 α mRNA by the PPAR δ agonist GW501516 in 32D cells (n=4). (B) Up-regulation of PPAR δ downstream genes (Angptl4 and Cpt1 α mRNA) by lipid mediators in 32D cells (EPA, eicosapentaenoic acid; DHA, docosahexaenoic acid; α -LA, α -linolenic acid; LA, linoleic acid, n=4-6). (C) Interference of EPA/DHA-induced PPAR δ signaling in 32D cells by the PPAR δ antagonist GSK3787 (n=4). (D) Alteration of PPAR δ mRNA expression by EPA/DHA in sorted three major myeloid cell fractions (CD11b⁺Ly6G^{high}F4/80^{low} mature neutrophils,

CD11b⁺Ly6G^{dull}F4/80^{low} immature neutrophils, and CD11b⁺Ly6G^{dull}F4/80^{high} monocytes/macrophages) from steady-state BM (n=3-7). Combined data of at least three independent experiments are shown. ns: not significant. Data are mean±SEM. *p<0.05, **p<0.01, ***p<0.001 (Student's t test and ANOVA).

Supplemental Figure 11. BM data in G-CSF mobilization experiments with EPA treatment related to Figure 6B-C.

BMNCs, LSK, and CFU-Cs in G-CSF mobilization experiments in the FFD condition in (A) WT mice treated with EPA (n=8) and (B) chimeric mice with PPAR $\delta^{+/+}$ or PPAR $\delta^{+/-}$ BM treated with EPA (n=4-6). Combined data of at least three independent experiments are shown. Data are mean±SEM. *p<0.05 (Student's t test and ANOVA).

Supplemental Figure 12. Expression and function of Angptl4 in G-CSF mobilization.

(A) Angptl4 protein level in plasma after eight doses of PBS/BSA or G-CSF (n=6). (B) Angptl4 mRNA expression in sorted BM major myeloid cell fractions (CD11b⁺Ly6G^{high}F4/80^{low} mature neutrophils, CD11b⁺Ly6G^{dull}F4/80^{low} immature neutrophils, and CD11b⁺Ly6G^{dull}F4/80^{high} monocytes/macrophages) after eight doses of PBS/BSA or G-CSF treatment with or without the PPAR δ agonist GW501516 (n=3). (C) Alteration of Angptl4 and Cpt1 α mRNA in BM cells during G-CSF mobilization with the PPAR δ agonist GW501516 in mice fed with ND or FFD (n=5). (D) BM data (BMNCs, LSK, and CFU-Cs) in G-CSF mobilization experiments in WT mice treated with the anti-Angptl4 antibody 3F4F5 (n=3-7). Combined data of at least three independent experiments are shown. ns: not significant. Data are mean±SEM. *p<0.05, **p<0.01, ***p<0.001 (ANOVA).

Supplemental Figure 13. Modulation of BM vascular permeability during G-CSF mobilization by the PPAR δ agonist.

BM vascular permeability assessed by Evans blue dye concentration in BMEF during G-CSF mobilization with or without the PPAR δ agonist GW501516 (n=5-9). Combined data of three independent experiments are shown. Data are mean±SEM. *p<0.05 (ANOVA).